Vision Research 158 (2019) 221–236

Contents lists available at ScienceDirect

Vision Research

journal homepage: www.elsevier.com/locate/visres

Full Length Article

A shape-level flanker facilitation effect in contour integration and the role of shape complexity

Christopher Gillespie*, Dhanraj Vishwanath

The University of St Andrews, Scotland, UK

ARTICLE INFO

No. of reviewers - 2

Keywords:
Contour integration
Object detection
Complexity
Perceptual grouping
Figure-ground organization
Shape
Pictures

ABSTRACT

The detection of an object in the visual field requires the visual system to integrate a variety of local features into a single object. How these local processes and their global integration is influenced by the presence of other shapes in the visual field is poorly understood. The detectability (contour integration) of a central target object in the form of a two dimensional Gaborized contour was compared in the presence or absence of nearby surrounding objects. A 2-AFC staircase procedure added orientation jitter to the constituent Gabor patches to determine the detectability of the target contour. The set of contours was generated using shape profiles of everyday objects and geometric forms. Experiment 1 examined the effect of three types of congruencies between the target and two flanking contours (contour shape, symmetry and familiarity). Experiment 2 investigated the effect of varying the number and spatial positions of the flankers. In addition, a measure of shape complexity (reciprocal of shape compactness) was used to assess the effects of contour complexity on detection. Across both experiments the detectability of the target contour increased when the target and flanker had the same shape and this was related to both the number of flankers and the complexity of the target shapes. Another factor that modulated this shape-level flanker facilitation effect was the presence of symmetry. The overall results are consistent with a contour integration process in which the visual system incorporates contextual information to extract the most likely smooth contour within a noise field.

1. Introduction

Detecting an object in a scene is a complex process that involves both local and global processing of visual information. At the level of a single object, a large number of studies have determined that mid-level shape features such as symmetry (Attneave, 1954; Baylis & Driver, 2001; Friedenberg & Bertamini, 2000; Mach, 1885, 1959; Machilsen, Pauwels, & Wagemans, 2009; Treder, 2010; van der Helm & Leeuwenberg, 1996, 2004; Wagemans, 1995; Wright, Makin, & Bertamini, 2017), part/whole relationships (Bertamini & Farrant, 2005; Hoffman & Singh, 1997; Keane, Hayward, & Burke, 2003; Rensink, O'Regan, & Clark, 1997), contour convexity/concavity (Bertamini & Wagemans, 2013; Huttenlocher & Wayner, 1992; Kanizsa, 1976; Koffka, 1935) and the shape aspect-ratio (Regan & Hamstra, 1992; Zusne & Michels, 1962a, 1962b) affect the detection of an object.

On the other end of the spectrum, the detectability of the target can be affected by the parameters of observation. For instance, the viewpoint from which an observer looks at an object (Jolicoeur & Milliken, 1989; Koenderink & Van Doorn, 1979; Moses, Ullman, & Edelman, 1996; Palmer, Rosch, & Chase, 1981; Tarr & Pinker, 1989; Vetter & Poggio, 1994) and the task-relevant allocation of spatial attention (Baylis & Driver, 1989, 1992; Carrasco, Ling, & Read, 2004; Duncan, 1984; Kravitz & Behrmann, 2011; Levin & Simons, 1997; Martinez, Ramanathan, Foxe, Javitt, & Hillyard, 2007; Mcmains & Somers, 2004; Posner, Snyder, & Davidson, 1980) have both been shown to be instrumental in determining how readily an object is detected.

Objects are often found as groups or ensembles in the environment, with varying spatial proximity and differing degrees of similarity and dissimilarity among the constituent attributes of the objects. A range of studies have examined how this might be relevant to the detection of a single object, group of objects or their constituent attributes. The most well known effect of the presence of other object on the detection of a target object is crowding. This is where the detection of a target's attributes (e.g. orientation, identity) is often be hampered by the presence of similar objects in spatial proximity (Bouma, 1970; Pelli & Tillman, 2008; Petrov, Popple, & Mckee, 2007; Stuart & Burian, 1962; Toet & Levi, 1992). In contrast, nearby objects can also enhance detection, for example, the detection of a low-contrast target object (Gabor patch) becomes more efficient when paired with other higher contrast flanking Gabor patches (Cass & Spehar, 2005; Chen & Tyler, 2001; Freeman, Sagi, & Driver, 2001; Huang & Hess, 2007; Polat & Sagi, 1993; Woods, Nugent, & Peli, 2002).

* Corresponding author at: School of Psychology, Philosophy and Language Science, University of Edinburgh, Edinburgh, UK.
E-mail address: Christopher.Gillespie@ed.ac.uk (C. Gillespie).

https://doi.org/10.1016/j.visres.2019.02.002
Received 20 June 2018; Received in revised form 14 February 2019; Accepted 16 February 2019
Available online 08 March 2019

The presence of information shared among neighboring objects can also potentially contribute to enhanced detection. For example, faster detection is often achieved when multiple instances of redundant information are available either inter- and intra-modally (Ben-David & Algom, 2009; Krummenacher, Muller, & Heller, 2001, 2002a, 2002b; Miller, 1982; Todd, 1912). At a larger spatial scale, global groupings of discrete objects facilitate judgements about the mean global value of common features (such as set size/orientation of multiple objects) in such a way that it has been suggested that the visual system actively encodes 'ensemble' properties of objects when grouped together–as opposed to encoding only properties of each object individually (Alvarez & Oliva, 2008; Alvarez, 2011; Ariely, 2001; Chong & Treisman, 2003; Dakin & Watt, 1997). This suggests a joint encoding of object properties at some level of processing.

Moreover, the ability to learn how to discern similarities and differences between visual regions is sensitive to prior exposure to simultaneously presented sets of visual objects. One example of this was identified by Mundy, Honey & Dwyer (2007, 2009). When two subtly different patterns (say, A and B) were presented together to observers (A + B), future discrimination between the two patterns was better than if there was prior exposure to the individual patterns alone (A + A, B + B). In other words the simultaneous rather than successive pre-exposure of two stimuli contributes to better discrimination between these two stimuli in the future.

Similarly, relative locations of two or more objects with specific features can also be significant. For example, symmetries in two objects can create additional inter-object symmetries which observers can detect in their own right (Baylis & Driver, 1995, 2001; Bertamini, 2010; Koning & Wagemans, 2009; van der Helm & Treder, 2009).

In this study, we aimed to examine the effects on target shape detectability of the presence of additional objects in the visual scene and gain an understanding about the levels of processing (high, mid or low) that any such effects might occur. In order to do this, we drew on work in contour integration which allowed us to manipulate both low-, high- and mid-level attributes relevant for object detection.

1.1. Contour integration

In order to generate the percept of a whole object, the visual system must first extract and organize the most basic local visual features (e.g., luminance, contrast and orientation) which form the elements of shape contours (Hubel & Wiesel, 1962, 1959; Marcelja, 1980) into a single discrete object. Contour integration is the process by which it is believed that outputs of low-level contrast and orientation selective units are combined in order to recover the profile shape of objects in the visual scene. Contour integration is thought to rely on the mechanisms of perceptual grouping in which unitary elements in the visual field are grouped together on the basis of similarity along some dimension such as colour, shape or orientation (Attneave, 1954; Wertheimer, 1923; Wallach, 1935; for a recent review, see Wagemans et al., 2012). Many studies have examined how similarities and differences in local dimensions or features detemine perceptual grouping (Barlow & Reeves, 1979; Beck, Rosenfield, & Avry, 1989; Field, Hayes, & Hess, 1993; Loffler, 2008; Smits, Vos, & van Oeffelen, 1985). Studies have also examined how grouping of local elements into a contour is further modulated by features arising on a larger scale. Factors such as the convexity or curvature of the contour (Bertamini & Wagemans, 2013), contour closure (Elder & Zucker, 1993; Gerhardstein, Tse, Dickerson, Hipp, & Moser, 2012; Kovacs & Julesz, 1993), symmetry (Machilsen et al., 2009); shape familiarity and predictability (Nygard, Sassi, & Wagemans, 2011; Sassi, Demeyer, & Wagemans, 2014; Sassi, Vancleef, Machilsen, Panis, & Wagemans, 2010; Sassi, Machilsen, & Wagemans, 2012) have all been shown to affect grouping or contour integration.

One of the main methodological approaches used to examine some of these issues has been a paradigm in contour integration introduced by Field et al. (1993). Here an observer attempts to detect a contour segment or shape contour defined by spatially separated oriented Gabor elements embedded in a noise field of similar randomly oriented Gabor patches. We reasoned that this method could be extended to examine the main questions of this study, namely the effect on the detection of a target object (shape contour) of the other objects (target contours) in spatial proximity. This contour integration paradigm would allow us to use low level feature manipulations to measure detection sensitivity of target objects in the presence of other obects while also controlling mid- and high-level factors such as symmetry, recognizability, and shape complexity.

While previous studies have mostly focused on the effects of similarity and variation between multiple features or objects across the visual field, there has been very little research on whether the presence of neighbouring objects can influence the underlying processing of the shape or objects being perceived. One example that suggests that the presence of multiple objects could have an effect on lower level processing is a study investigating features and attention by Stojanoski and Niemeier (2007). They used the gaborised contour paradigm to determine whether information derived from directing an observer's attention to a target contour had an effect on the detection of unattended contours presented simultaneously that contained similar or dissimilar features to the attended target. They determined that observers were more readily able to detect the second unattended contour in the periphery when both contours shared a common feature.

In contrast, here we were interested in examining whether the presence of contours in the immediate surround of a central target contour facilitated or impeded the contour integration of the central target. We were specifically interested in how any such facilitation/inhibition was modulated by factors such as symmetry, shape familiarity and contour complexity.

1.2. Experimental summary

The experiments consisted of detecting a Gaborized target contour embedded in a random Gabor noise field in the presence or absence of other flanking contours. The first experiment investigated the effect of flanking gaborised contour shapes on the detectability of a central (gaborised) target contour, depending on whether the target and the flanking objects were similar or dissimilar (see Fig. 7) The contours were chosen to also evaluate the roles of symmetry, familiarity and shape complexity. The second experiment examined the role of flanker numerosity and the relative positioning of the flanker objects, specifically, whether they were positioned in the cardinal positions (up, down, left and right) or at diagonal positions relative to the central target contour.

2. Experiment 1

2.1. Methods

2.1.1. Participants

In total, 26 paid volunteers participated in the experiment, but 7 did not complete the experiment to a level that would provide a full data set suitable for analysis (2 could not perform the task and 5 did not turn up for a second session). Of the 19 participants who performed the full experiment, 14 were paid undergraduate volunteers and 5 were post-graduate students or members of university staff who performed the task without payment. 17 of the participants were female. The age range was 17–50 years. Each participant performed two sessions (1 h per session). Two breaks were provided at approximately 1/3 and 2/3 of the way through the session for as long as the participant wished. All participants had normal or corrected-to-normal vision (defined as an acuity of 20/30 on a Snellen chart). Ethics was granted by the St Andrews University Teaching and Research Ethics Committee.

2.1.2. Apparatus and software

Stimuli were presented on a Dell 2407WFP LCD display with a resolution of 1920 × 1200 with a refresh rate of 60 Hz. The viewing

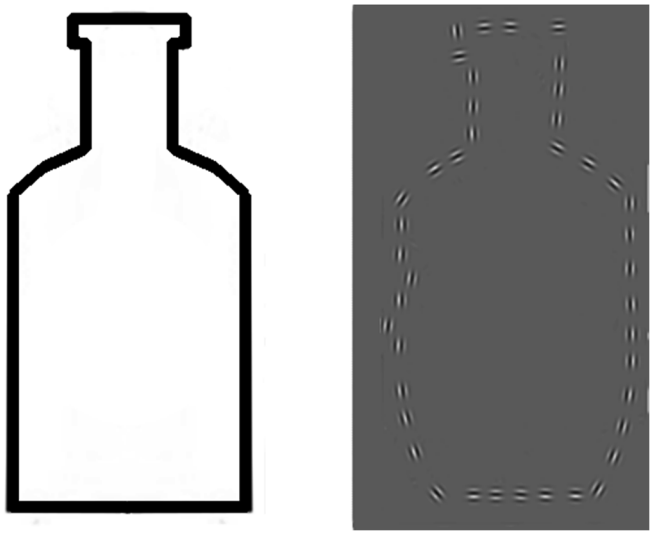

Fig. 1. Methodology for generating Gaborized contours. The Gaborized contour stimuli were generated by combining pre-set shapes with a group of Gabor patches. The methodology for creating Gaborized contours involved taking a smooth shape and automatically placing Gabor patches at quasi-random and jittered intervals along the path of the shape (Demeyer & Machilsen, 2012). In the base version of the Gaborized contour, individual patches had their orientations aligned with the orientation of the line of the shape. In the experiment, noise was added to Gaborized contour as described in Fig. 2 below.

distance was 57 cm. Participants viewed the screen from a chin/head rest. The experiment was implemented using Matlab (Mathworks, Inc.) and the psychophysics toolbox utilities (Brainard, 1997). Statistics were performed in R (Development Core Team, 2008) and presented using Gnuplot (Williams & Kelley, 2011).

2.1.3. Stimuli

The stimuli were created using the Grouping Elements Rendering Toolbox (Demeyer & Machilsen, 2012) based on the Matlab programming language. The staircase procedure used to present the stimuli for each trial was run using the Palamedes Toolbox (Prins & Kingdom, 2001). The stimuli consisted of two components: A set of sine waves windowed by a Gaussian envelope, known as a Gabor patch, and a generating shape combined with a set of Gabor patches to generate the stimuli presented to the observers (Fig. 1).

The Gabor patches consisted of a sine wave luminance profile of frequency 2.5 cycles/deg within a 2-dimensional Gaussian envelope that subtended 24 arc minutes. The phase of each Gabor patch was randomised by 90 deg. The panel was primarily populated with a field of randomly positioned, non-overlapping, randomly oriented Gabor patches (referred to as the noise field). The average initial minimum spacing between Gabor patches (prior to density adjustments) in the noise field was around 1 degrees visual angle (Fig. 2).

To create the target contours, a set of generating shapes was combined with a number of Gabor patches (Fig. 3). The generating shapes are presented in Fig. 4. The shapes were chosen to encode two factors: The presence of bilateral symmetry, and observer familiarity with the object shape. Four groups were generated consisting of familiar and bilaterally symmetric, unfamiliar and bilaterally symmetric, familiar and asymmetric; and unfamiliar and asymmetric contours.

Another factor that was considered, which would be particularly relevant to this contour integration paradigm, is the inherent differences in difficulty in perceiving a contour due the overall complexity of the shape (number of protruding parts, degree of curvature, etc.). This can be seen in Fig. 5, in which changes to the local orientation of a circle increases the complexity of the shape, which in turn reduces the likelihood of the shape being recognised as a circle. To account for this,

Fig. 2. Addition of orientation and positional noise to Gaborized contours. Left Panel: An example of Gabor patches delineating the contour. The relative spacing was varied by randomizing the distance between sequential Gabor patches by up to two wavelengths of the patches used. Finally, orientation jitter was used to decrease the alignment of adjacent Gabor patches. Right Panel: The absolute position and orientation was randomized for Gabor patches associated with the noise field. The relative positions of Gabors in the noise field were adjusted so as to remove any density cues.

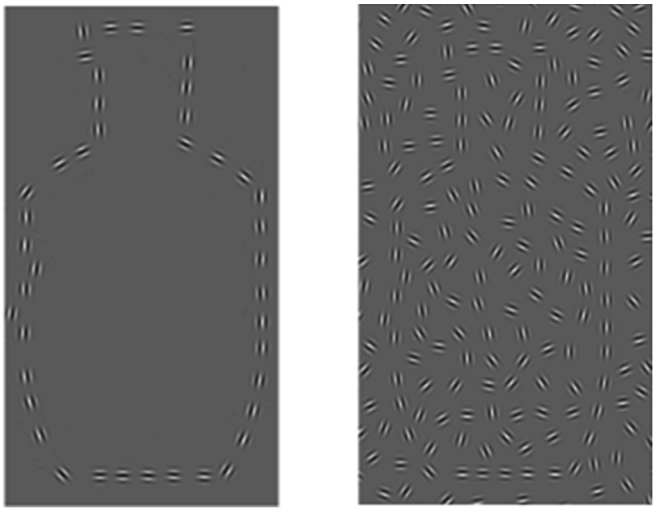

Fig. 3. A target Gaborised object embedded in noise. To disrupt the visibility of the target contour the Gaborized contour (left panel) was presented embedded in a noise field of randomly orientated Gabor patches (right panel). The introduction of a Gaborized contour into a randomized noise field introduced potential differences in the local density of Gabor patches. These local density inconsistencies were assessed and removed using the Voronoi metric method specified in Demeyer & Machilsen, 2012, and validated in Machilsen, Wagemans, and Demeyer (2016) (see Section 2.1).

Fig. 4. Shapes used to generate target and flanker Gaborized contours. Four groups of generating shapes were created using outlines of everyday objects (e.g., fish, butterfly, Jug) and a set of geometric forms of varying regularity (e.g., Hexagon, non-regular curvilinear shapes). Group A (shape 1) consisted of bilaterally symmetric familiar shapes. Group B (shape 2) consisted of asymmetric familiar shapes. Group C (shape 3) consisted of bilaterally symmetric unfamiliar shapes. Group D (shape 4) consisted of asymmetric unfamiliar shapes.

Fig. 5. Cartoon demonstrating effects on shape complexity (compactness) in the context of Gaborized contours with added orientation noise. The left panel shows a Gaborized contour forming a circle. The middle and right panel show the same contour with increasing amounts of added orientation noise. The dotted lines in each case show the generating shape used to initially align gabors and to which orientation jitter is then added (noise). The greater the added noise, the larger the deviation of the implied smooth shape from the generating circle. Specifically, there is an increase in contour perimeter despite on-average same total area contained by the contour. This implies that the complexity of the shape (defined as the ratio of the perimeter of the shape to its area increases as orientation noise is added (left to right). Conversely the compactness of the implied contour decreases from left to right. For any given shape at a particular level of added orientation noise, we define a *Complexity Differential* as the difference between the complexity of the shape with added noise (e.g., middle or right panel) and the complexity of the base contour with no orientation noise added (left panel). For the purposes of this study, the Complexity Differential was estimated based on deriving a value for change in complexity per degree increase of orientation noise by using a manual procedure which used a selected range of stimuli generated for the experiment. For more details, see Appendices A–C.

a measurement of the complexity of each encoding shape was taken. Complexity is here defined as the reciprocal of shape compactness (Zusne & Michels, 1962a, 1962b, for a review on complexity/compactness as a measurement, see Montero & Bribiesca, 2009). Shape complexity/compactness is a dimensionless measure derived by comparing the overall area with the overall perimeter length of a contour (Eq. (1.1)).

$$C = \frac{P^2}{4 * \pi^2 * A} \tag{1.1}$$

Here C is the complexity of the shape, P is the length of the perimeter of the shape, and A is the enclosed area for the shape. The resulting number is a dimensionless ratio. The minimal value, 1, corresponds to the complexity of a circle in which a minimum length of contour is distributed along the maximum enclosed area.

The Complexity values for each generating shape tested are shown in Fig. 6. The shapes were chosen such that shapes for each factor (symmetry, familiarity) were distributed across the range of complexity values of 1–4.5, where feasible.

A set of approximately 20 Gabor patches were placed at intervals along the perimeter of the generating shape such that the orientation of these individual Gabor patches corresponded with the local orientation of the underlying generating shape (Fig. 3). The distance between Gabor elements was randomly selected from a range of values that varied between 0.5 and 2 wavelengths of the Gabor. Inspections were made of the subsequent Gaborized contours and minor adjustments (± 2 Gabor patches) were made if the resultant contour lacked corners or extrema.

The stimuli were presented on a grey rectangular panel (14 × 8 deg.) which was placed on an otherwise black screen. The Gaborized contours were then embedded in the noise field so that there was no overlap with the randomly orientated noise Gabor patches. The Gaborized flanker contours were embedded in a Gabor field whose Gabor patches were aligned vertically. This was to maintain visibility for more complex flanker shapes in visual periphery while still maintaining contour integration processes in both the target and flanker region.

The combination of Gaborized contour and the noise field introduced possible variations in the density of the overall panel of Gabor

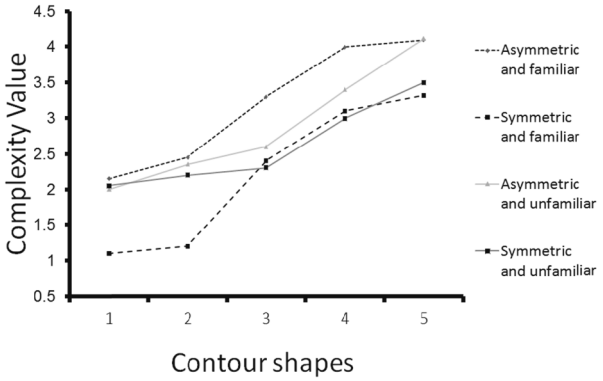

Fig. 6. The individual complexity values for the generating shapes. Shape Complexity (reciprocal of compactness) is plotted on the y-axis for each shape used as a target contour (x-axis). The groups of shapes presented contained a range of complexity values between the values of 1–4.5. This range varied approximately linearly though the full set of shapes.

gratings. To assess the presence of probabilistically significant density differences, and to subsequently adjust the relative locations of the set of Gabor patches, a method native to the stimuli generating program, GERT, was used. This employed a Voroni tessellation to isolate the immediate area surrounding each Gabor patch and trace it as a polygon. The surface areas for the polygons were computed and compared across both the noise field and the embedded contours to determine that the surface areas were reasonably uniform across the whole stimuli.

The detectability of the target contour was varied by adding orientation noise jitter to the individual Gabors making up the contour (Field et al., 1993). The amount of orientation noise jitter added across the set of Gabor patches was sampled from a uniform distribution. The maximum value such orientation jitter could take was the range of 90 to −90 deg away from alignment.

In these experiments the results are reported as the magnitude values (e.g., a range of 90 to −90 deg difference corresponds to a maximum magnitude of 180 deg). For example, 40 deg of jitter (−20 to 20) represented a highly visible contour with a low level of orientation noise, while 120 deg of jitter (−60 to 60) represented a contour of low visibility due to a high level of orientation noise.

The central Gaborized target contour was presented with and without additional flanking contours in one of the following configurations: (1) the control condition in which the target was presented alone (1) “No Flanker”; (2) the ‘Matching Flankers’ condition in which the shape of a target was paired with two flanking contours which had the same shape as the target; (3) the ‘Non-Matching Flankers’ condition presented the target flanked by two contours of a different shape than the target, but the same as each other. The flankers (when present) were displayed to the left and right of the target so their centroid aligned vertically with the target centroid, and the horizontal distance between centroids was approximately 4.7 arc degrees. Examples of these conditions are presented in Fig. 7.

2.2. Procedure

Each trial consisted of two stimulus presentations, a target-present panel and a target-absent panel. In the target-present panel the target was displayed centred on the vertical meridian. The target absent panel consisted of a randomised noise field with no embedded target, but the location of flankers was the same. In order to prevent any gross differences in perceived density of the two types of panels the average density of the target absent panels was generated by matching it to the value of the target present condition (Voronoi metric native to GERT). The number of Gabor patches in the target-present and target-absent panels was therefore the same. The density value was further used to create a set of 5 different inter-trial display panels for each set of

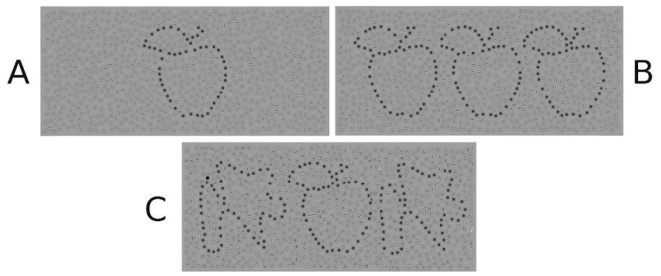

Fig. 7. Stimulus conditions in experiment 1. Diagrammatic representation of the three conditions in which the target was presented alone or in the presence of flankers. Note that the actual stimuli consisted of Gaborized contours embedded in noise. The three flanker conditions are (A) No Flankers: the control condition in which the target contour was presented alone; (B) Matching Flankers: the target contour was simultaneously presented with two flanking contours of the same shape; (C) Non-matching Flankers: the flanking contours are a different shape from the target.

presentation panels. These inter-trial display panels contained no contour information as they contained randomly positioned and orientated Gabor patches only.

The stimulus presentation sequence (Fig. 8) involved an initial fixation cross at the center of the main display panel (750 ms), followed by a fixation cross appearing at the upper or lower half of the overall panel. This was followed by the presentation of either a target-present or target absent stimulus panel for 500 ms. After this time, a fixation cross appeared at the opposite location (lower or upper panel) and was followed by either the target-absent or target-present panel (depending on what was previously shown). A circle was presented indicating to the participant to respond if the contour was present in either the upper or lower panel. Once a response was recorded an inter-trial display was presented for 700 ms and a central red circle was flashed (200 ms) to indicate the beginning of a new trial. The first presentation panel for any given staircase for each contour consisted of Gabor gratings aligned to the underlying generating shape (i.e. supra-threshold detectability). The degree of orientation noise was varied according to participant responses using a weighted 1-up 1-down staircase procedure targeting approximately a detection threshold of 67 percent (Kaernbach, 1991). Reversals only took place after the first 3 trials had been completed regardless of response. This was done to increase the efficiency of the experiment as at the lowest levels of noise the contours were clearly visible. The step size in the initial 3 trials was 16 degrees of noise. This large step size was intended to reduce the number of steps required to approach the detection threshold level. After the first 3 trials, step size was reduced to 4 deg. If the participant was incorrect at the lowest level of noise the level of noise remained the same during the first three trials. To extract the detection threshold, the staircase procedure varied the magnitude of the added orientation noise jitter until the participant was no longer able to detect the shape.

Each staircase was terminated after 15 reversals occurred for the individual contour and the threshold was calculated by taking the mean value over which the last 10 reversals took place. In circumstances where less than 15 reversals occurred by the end of 50 trials the individual staircase was terminated, if less than 8 reversals took place the staircase was removed from the dataset. Here, the detection thresholds corresponding to the absolute magnitude of orientation noise jitter present in the threshold stimulus. In other words, the larger the value, the more sensitive is the observer (detectability at higher levels of orientation noise).

A number of participants could not perform the task for all contour types (that is, for complex contours such as the cat their performance was around the lowest level of additional noise). Additionally, a number of contours staircases over-shot the detection threshold and did not return in the allocated number of trials. Two limits corresponding to detectability values of 30 and 160 were chosen and data that was above or below these values were discarded.

2.3. Data analysis

The detectability of the target-contour was analysed by taking the mean of detection thresholds and computing a $3 \times 2 \times 2$ ANOVA with flankers condition, bilateral symmetry, and shape familiarity as factors.

2.4. Results

First, we examine the mean detection thresholds averaged across all observers and across all contour types for the three experimental conditions (Matching Flankers, Non-Matching Flankers, No-flanker control) which are shown in Fig. 9. Then, we compare the underlying benefits of the additional factors on detection, Fig. 10 plots these detection thresholds as a function of the factor shape symmetry and shape familiarity. Finally, Fig. 11 plots the detection thresholds as a function of both shape symmetry as well as condition (Matching Flankers, Non-Matching Flankers, No-flanker control).

A $3 \times 2 \times 2$ factorial ANOVA was performed with the three factors of: flanker condition, bilateral symmetry, and shape familiarity. A Levine's test (Test statistic = 2.1289, $p = 0.322$) and Shapiro-Wilks tests (flanker condition ($W = 0.8$, $p = 0.46$); familiarity ($W = 1.63$, $p = 0.2$); and bilateral symmetry ($W = 1.19$, $p = 0.2761$) confirmed that the data was normally distributed and that the variance was homogenous across the factors in the experiment.

There was a main effect of the condition of flanker contour shape relative to the target contour shape ($F(2,36) = 8.215$, $p < 0.01$), where the overall mean threshold for detecting a target contour was lower (tolerance to orientation noise was higher) for the target contours in the Matching condition in comparison with the No-Flanker and Non-Matching condition; Fig. 9). The mean detection thresholds calculated on the basis of the symmetry/asymmetry factor combined across all flanker conditions (Fig. 10a) showed that there was an increase in the detectability associated with the presence of bilateral symmetry ($F(1, 18) = 4.72$, $p < 0.001$).

However, we found no effect of familiarity ($F(1, 18) = 5.513$, $p = 0.231$) (Fig. 10b). However, this outcome should be interpreted with caution, given that previous studies have found effect of familiarity (Sassi et al., 2014) and this could simply be due to interactions with other factors in our specific stimulus and experimental design

There were also significant interactions between symmetry and

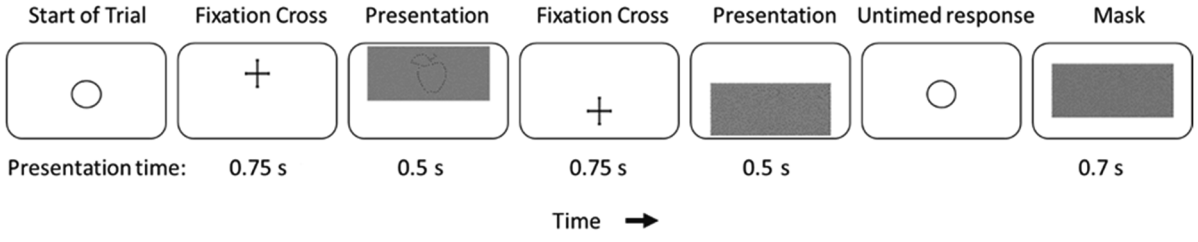

Fig. 8. The time course of a single trial. Each trial consisted of two sequential presentations, one in which a central Gaborized contour target was present and one in which it was absent (random order). The task was to determine in which interval the target was present.

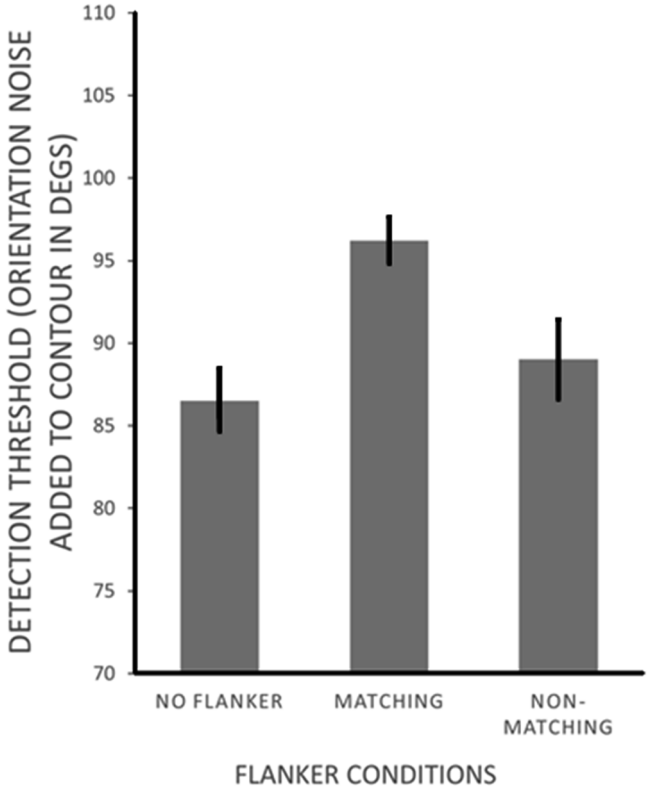

Fig. 9. Mean detection thresholds for the target contour for the flanker conditions. The detection thresholds (y-axis) are presented against each of main conditions run during the experiment (x-axis). The plotted conditions is the target-flanker conditions, which contained three conditions (e.g., control, matching and non-matching). The plotted data are the magnitude of orientation jitter added to a central target contour at a detection threshold of 67% correct averaged over all participants (n = 19). Error bars represent the standard error of the mean.

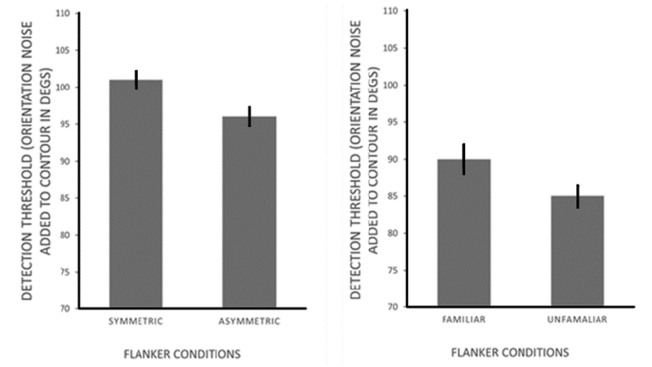

Fig. 10. Mean detection thresholds for the target contour plotted as a function of the contour symmetry (left) and contour familiarity (right). The detection thresholds (y-axis) are the magnitude of orientation jitter added to a central target contour at a detection threshold of 67% correct averaged over all participants (n = 19). Error bars represent the standard error of the mean.

flanker condition ($F(2, 36) = 21.72$, $p < 0.001$) as seen in the data in Fig. 11 which plots detection thresholds as a function of both flanker condition and presence of symmetry. In both the Matching and Non-Matching flanker conditions, the symmetric contours had higher detectability, while the difference between the two for the control no flanker condition is smaller and in the opposite direction.

There was also a significant interaction between the symmetry and familiarity conditions ($F(2, 36) = 32.39$, $p < 0.001$) shown in Fig. 11 The interaction may be due to an unavoidable confound that (a) symmetry itself was being used as a form of familiarity, or (b) that symmetric shapes are generally familiar. There was therefore a marginally significant three way interaction between symmetry, condition and familiarity ($F(2, 36) = 3.838$, $p < 0.05$).

These results showed that there was an increased detectability when a target contour was paired with flankers of the same generating shape as well as greater detectability for symmetric and recognisable shapes. This also suggested that there was an enhanced facilitory effect when both symmetry and additional flankers were present within a trial.

3. Experiment 2: Effect of flanker numerosity and alignment with target on contour detection

3.1. Methodology

3.1.1. Participants

Experiment 2 was performed by 18 participants who were paid volunteers (£5 for each hour). 16 were undergraduate students and 2 were postgraduate students. 13 of the participants were female. 9 of the participants had performed experiments for the previous experiments. 1 participant was unable to perform the task and their data was discarded. The participants were in the age range of 17–50. All observers had normal or corrected-to-normal vision.

3.1.2. Apparatus

The apparatus was identical to that in Experiment 1.

3.1.3. Stimuli

The stimuli were generated in an identical way to Experiment 1. The set of shapes used to generate the Gaborized contours were a subset of the initial experiment (Fig. 12) and consisted of symmetric shape only. We used this subset since the symmetric shapes yielded the strongest flanker facilitation effect. Experimental conditions were created by pairing a target contour in the centre of the presentation region with a number of flanking contours, Fig. 13). The experimental conditions consisted of a target contour paired with 0, 1, 2, 3, or 4 flanking contours with the same shape. Two sets of relative locations were generated. One consisting of flanking contours presented in the adjacent locations above/below and left/right of the target contour (cardinal) and the other, in one of the four corners (diagonal) of the presentation panel. These are shown in Fig. 13. For each condition there were a number of possible combinations of locations and flanking contours (i.e., a single flanker presented could be in one of four positions around the target contour. During the trials the possible locations were randomised across all possible combinations. For any given staircase the participant was presented a single number of flanking contours (e.g., 0, 1, 2, 3 or 4) that were randomly arranged spatially relative to the target contour.

3.2. Procedure

The procedure was similar to that in the previous experiment except for the following: The time of presentation was reduced from 500 ms to 200 ms to decrease the likelihood of making saccades to flanking regions. All flankers (when present) were matched to the shape of the target, i.e., the Non-Matched flanker condition was not tested here as were interested in the flanker facilitation effect of the Matched flanker condition and the role of numerosity. Each participant performed two sessions of about 1 h. In the first session they were tested with the flanking contours in the cardinal positions, in the second they were tested in the diagonal positions. Two breaks were provided during each session approximately 1/3 and 2/3 of the way through the experiment and the duration of the break was determined by the participant.

Each stimulus condition (e.g., target with matching flankers) was presented with between 0 and 4 flankers in either a cardinal (e.g., up, down, left, right positions relative to the target) or diagonal (e.g., in upper/lower left or right corners relative to the target). In the cases

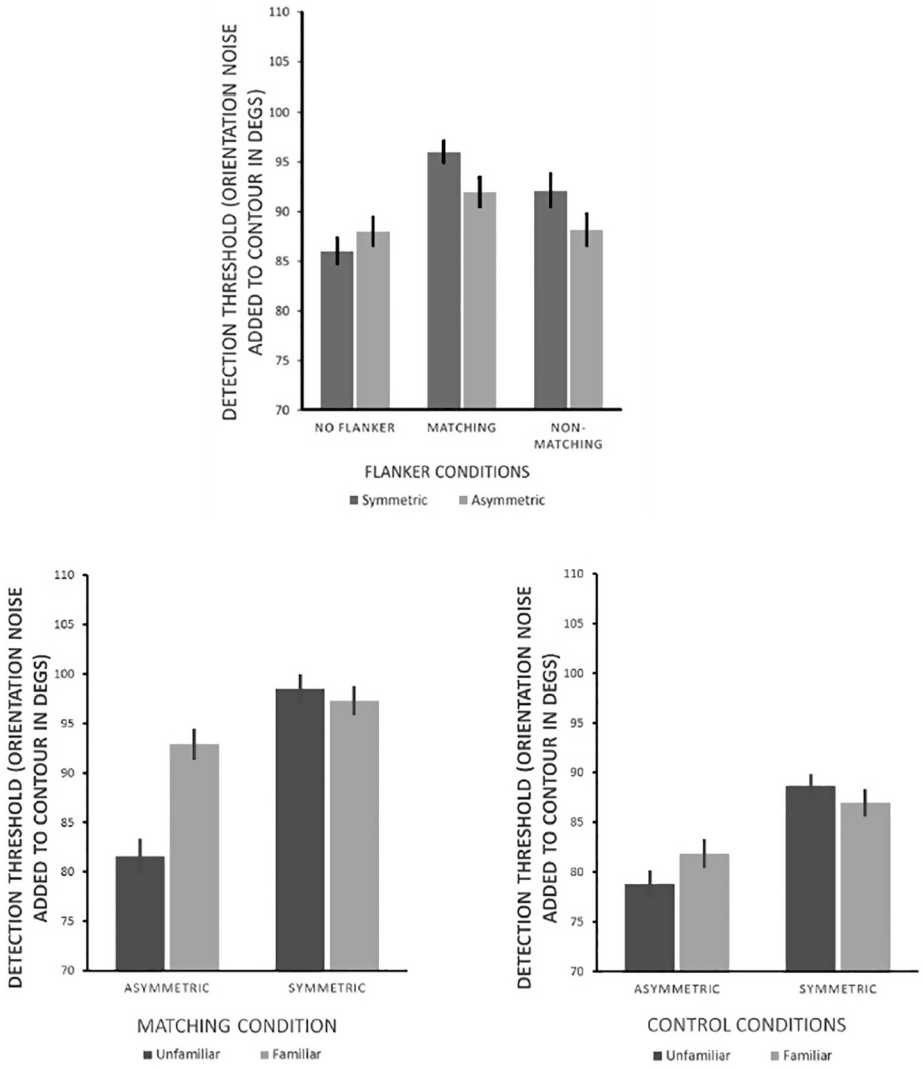

Fig. 11. Mean detection thresholds for the target contour as a function of flanker conditions and symmetry. Top graph: The detection thresholds (y-axis) are plotted against two of main factors in the experiment (x-axis). Dark grey bars are for the asymmetric contours and the light grey bars are for the symmetry contours. The plotted data are the magnitude of orientation jitter added to a central target contour at a detection threshold of approximately 67% correct averaged over all participants (n = 19). Error bars represent the standard error of the mean. Bottom graphs: Graph showing interaction between the factors 'familiarity' and 'symmetry' for the matched flanker (left graph) and control (right graph) conditions respectively.

Fig. 12. Target shapes used in Experiment 2. All shapes consisted of bilaterally symmetric, familiar shapes.

where there were multiple possible locations for a condition (for instance, a single flanker could be in one of four locations) these possible locations were randomised pre-experiment. In total each subject was tested on 25 staircases per experimental condition (cardinal, diagonal).

3.3. Results

The mean detection threshold was determined by averaging over all the target contour shapes for each level of flanker numerosity. The mean values averaging across all observers are shown in Fig. 14. In both cardinal and diagonal positions the lowest target detectability was found when the target contour was presented without any flanking contours (control condition). An increase in the number of flanking contours corresponded to an increase in the detectability of the target contour. For both flanker conditions (diagonal and cardinal) the addition of flankers had a significant effect on detectability (diagonal: $F(4, 56) = 3.194$, $p < 0.05$; cardinal: $F(4, 72) = 4.9$, $p < 0.01$). The increase in facilitation with flanker numerosity appeared to be generally monotonic and start to plateau at 4 flankers for both arrangements of flankers. This suggested that addition of more flankers would have a diminishing effect on facilitation. The planned pairwise comparisons using a Tukey test showed a significant increase in detectability relative to control condition for both the flanker arrangements. Both the Levene's test and Shapiro-Wilks tests confirmed that both flanker arrangements satisfied the homogeneity of the variance and normality. For the cardinal arrangement, significant pairwise differences from control were found for the single ($p = 0.04$), three ($p < 0.001$) and four ($p < 0.001$) flanker conditions, while for the diagonal arrangement, significant pairwise differences from control were found for single ($p < 0.05$), two, ($p < 0.005$), three ($p < 0.01$) and four ($p < 0.001$).

The overall detectability was greater for the diagonal flanker placements though this is likely due to a practice effect as the cardinal and diagonal conditions were examined in consecutive sessions. This is particularly likely because the same difference is also seen in the control (No-Flanker) condition.

4. Discussion

The present set of experiments was designed to examine whether the detectability of a Gaborized contour was affected by the presence of flanking contours with similar or dissimilar shape. This was established by measuring contour detection thresholds in the presence of

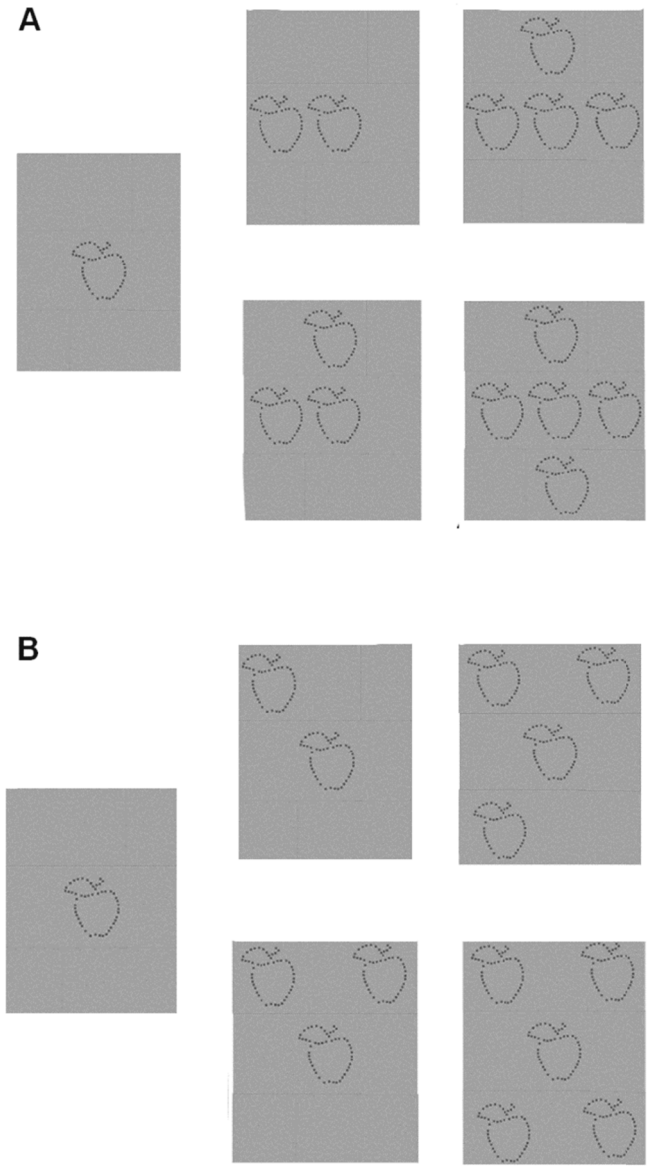

Fig. 13. Stimulus conditions presented to examine the role of numerosity and relative alignment of flanking contours on target detectability. In previous experiments the flankers were placed in a region of 4.5 by 14 arc degrees. To accommodate for the increase in flanker number and changes in location the region was increased to 14 by 14 arc degrees.

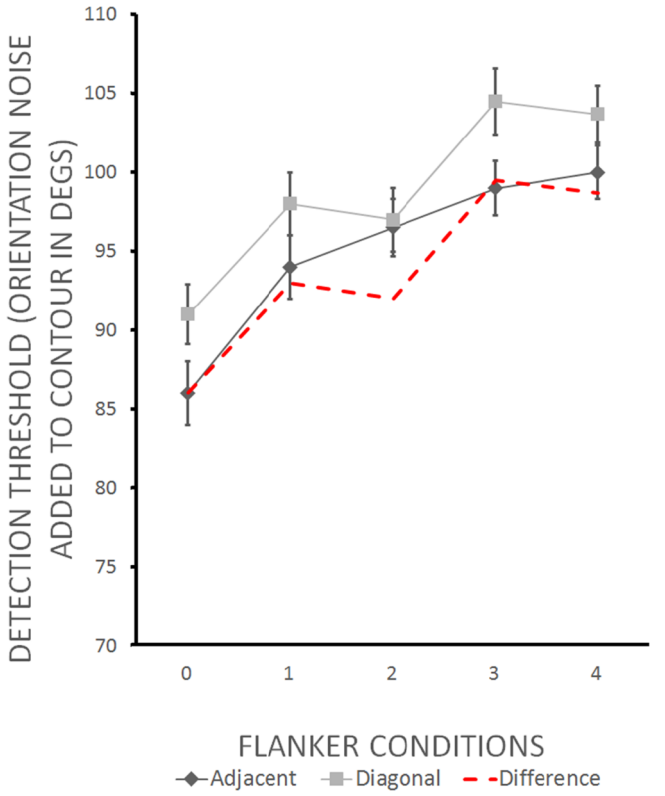

Fig. 14. The mean detection thresholds for the target contour as a function of the numerosity of flankers. Diamond symbols are for the cardinal locations and diagonal symbols are for the diagonal locations. The plotted data are the detection threshold (magnitude of orientation noise tolerated) averaged over all participants (n = 18/n = 15). Error bars represent the standard error of the mean. Since the diagonal orientation was tested after the cardinal orientation, the vertical offset is likely due to practice effects. The red dashed line is the data for the diagonal locations re-plotted normalised to the threshold for the control no-flanker (0) condition. (For interpretation of the references to colour in this figure legend, the reader is referred to the web version of this article.)

orientation noise added to individual Gabors making up the contour. Thresholds were assessed in terms of the amount of orientation noise present at detection threshold.

The primary result of both experiments was that adjacent flankers with the same generating shape as the target contour facilitated the detection of the target contours. In addition, this shape-level flanker facilitation effect was sensitive to the number of the contours; as the number of flankers increased, there was an increase in the facilitation though this increase appeared to asymptote at flanker numerosity between 3 and 4. We found no systematic difference in facilitation due to increased numerosity with respect to the location of the flankers relative to the target (adjacent or diagonal), although the pattern of results was a bit more variable for the diagonal arrangement.

There are two conceivable explanations for the shape-level flanker facilitation effect. Firstly, the flankers may simply be facilitating contour detection via a sort of top-down global flanker shape search template that facilitates the detection of the underlying contour even in the presence of noise (Born, 2000; Bundesen, Habekost, & Kyllingsbaek, 2005; Desimone & Duncan, 1995; Olivers, Peters, Houtkamp, & Roelfsema, 2011; Tünnermann, Born, & Mertsching, 2013). Under this explanation, the observer is applying a cognitive strategy of searching for target contour shape within the noisy field that matches the global shape template.

We found no significant de-facilitation with non-matching contours. In fact, mean values showed that detectability was slightly better than control for the non-matched flanker condition, although not significantly so (Figs. 9 and 11). Moreover, since the experiments were set up so that targets were suprathreshold at the beginning of the experiment, observers would have noticed that there was often not a match between target contour and flanking contour, thus a cognitive strategy of looking for a matching contour would have been inefficient and would have yielded less sensitivity for the non-matched flanker condition.

An alternative view is that the visual system is not searching for a match to a template but rather that the presence of flanking contours facilitates the visibility of any plausible contour within the Gabor noise field. In other words, when flanking contours are present, shape level mechanisms facilitate contour formations by rendering specific arrangements of Gabors more probabilistically likely to represent a smooth contour. Here, rather than attempting to match Gabor patterns in the noise field to a particular global shape template, it may be that the visual system is primed to integrate contour segments within the central noise field, and any transiently integrated contour is deemed

more likely to represent a true contour signal if that contour matches some of the specific features of the supra-threshold contours in the flanking regions (e.g., symmetry, degree of curvature, or presence of curvature minima/maxima). Hence the visual system may be involved in a sort of probabilistic cue-combination process based on likelihood (Machilsen & Wagemans, 2011). Note that this could be conceivably construed as the application of local "templates" operating at the perceptual rather than cognitive level.

The numerosity effect is also difficult to interpret under the top-down search template hypothesis (it is hard to see how more examples of the same template should make a difference), although perhaps an appeal can be made to the relative strengthening of the resolution of template with greater numerosity but subject to inherent attentional set size limits of 3–4 items (Baylis & Driver, 1989,1992; Evans et al., 2011; Maxfield, 1997; Pashler, 1994; Posner et al., 1980; Pylyshyn & Storm, 1988; Yantis, 1992; Yarbus, 1961). Alternatively, for the probabilistic contour integration account, presence of a greater number of flankers may increase likelihood of contours of certain features (asymptoting to certainty), for example, the certainty of an ensemble feature value (Alvarez & Oliva, 2008; Alvarez, 2011; Ariely, 2001; Chong & Treisman, 2003; Dakin & Watt, 1997).

While the present results cannot conclusively determine which model (top-down global search template vs. post-integration contour likelihood) best explains the observed facilitatory behaviour, the pattern of results suggest enhancement of contour integration based on perceptual shape-level factors rather than whole-shape identity or matching that operate in conjunction with cognitive mechanisms, though this needs to be explored further.

One important issue is whether the baseline detectability of a target contour is shape dependent. In other words, is the tolerated level of noise in the threshold detection paradigm used in this study independent or dependent on basic attributes of the shape of the underlying contour (such as degree of curvature, number of curvature minima/maxima, numbers of parts, etc.)? One way to capture some of these factors into a single measure, as mentioned previously (see Section 2.1), is in terms of the compactness (complexity) of the shape. This is a unit-less measure that is the ratio of the perimeter length to the bounded area of the shape. Figs. 15 and 16 plot detection thresholds for each individual shape as a function of the shape complexity value (reciprocal of compactness; see Section 2.1). Fig. 15 plots the detection thresholds as a function of complexity in the control (no-flanker) condition, while Fig. 16 plots thresholds for the matching flanker condition. We found no statistically significant correlation between detection thresholds and shape complexity/compactness for either the experimental (flankers present) or control flakers absent condition ($r = -0.053$, $p = 0.83$, 95% CI: -0.48 $+0.4$; $r = -0.145$, $p = 0.54$, 95%CI: -0.55 $+0.32$). One possible reason for this is that addition of orientation noise will likely have very different effects depending on the shape of the contour. For example, there could be different effects of a few degrees of random orientation jitter for a shape that has a complex boundary with many high curvature segments compared to one that has a simpler, lower curvature boundary. Moreover, this can bear on the question of whether or not the flanker facilitation effect occurs at the level of a top down global matching an already integrated contour to a plausible closed shape, or whether the facilitation actually acts at the local level of the integration of contour segments themselves. For this and other reasons, assessing detectability directly as a value of orientation noise level may not adequately capture the nature of the facilitation and at what level such facilitation is occurring.

Consider the detection of a Gaborised target in the shape of a cat. The cat is represented by discrete Gabor elements scattered along the boundary of the cat shape. In the context of detection, contour integration or contour search could be facilitated in two ways– if one knows the likely specific arrangement of the Gabors of a target (e.g., attentional template with information about direction of tail/ size head/relations between each part) contour integration mechanisms might attempt to integrate a contour of a specific shape within the noise field. If the contour is indeed implied by the Gabor orientations, the template might make the contour integration process more tolerant to orientation noise. Here, the contour integration process can be seen as happening on the basis of a pre-existing template for attempted contour integration. If the template does not match the contour implied by the (orientation jittered) Gabors, integration is not facilitated. However, this model does suggest that if the shape of the flankers is different from the target, then there could plausibly be a suppression due to a mismatch between the template shape and the local orientations of the Gabors-something we did not find.

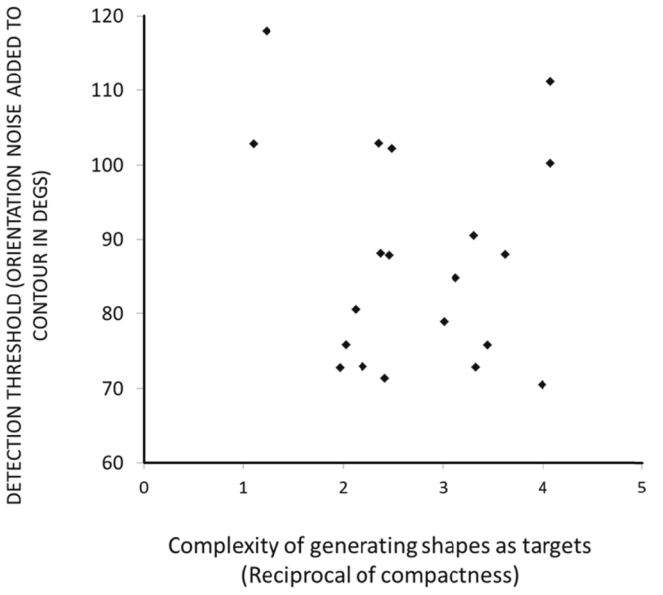

Fig. 15. The mean detection threshold as a function of the complexity of the shape of the target contour in the control condition averaged across all observers for each shape tested. The plotted data is the detection thresholds (y-axis) from the control condition versus the complexity of the shape of the contour (x-axis).

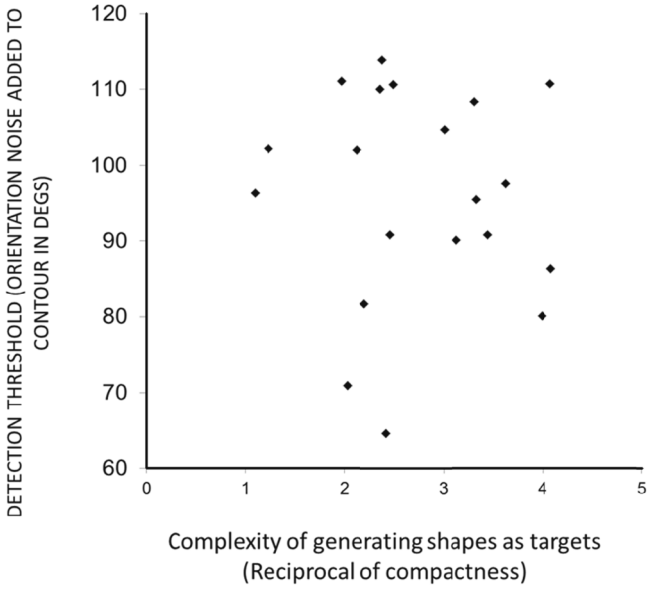

Fig. 16. The mean detection threshold as a function of the complexity of the shape of the target contour in the matched flanker condition averaged across all observers for each shape tested. The plotted data is the detection thresholds (y-axis) from the control condition versus the complexity of the shape of the contour (x-axis).

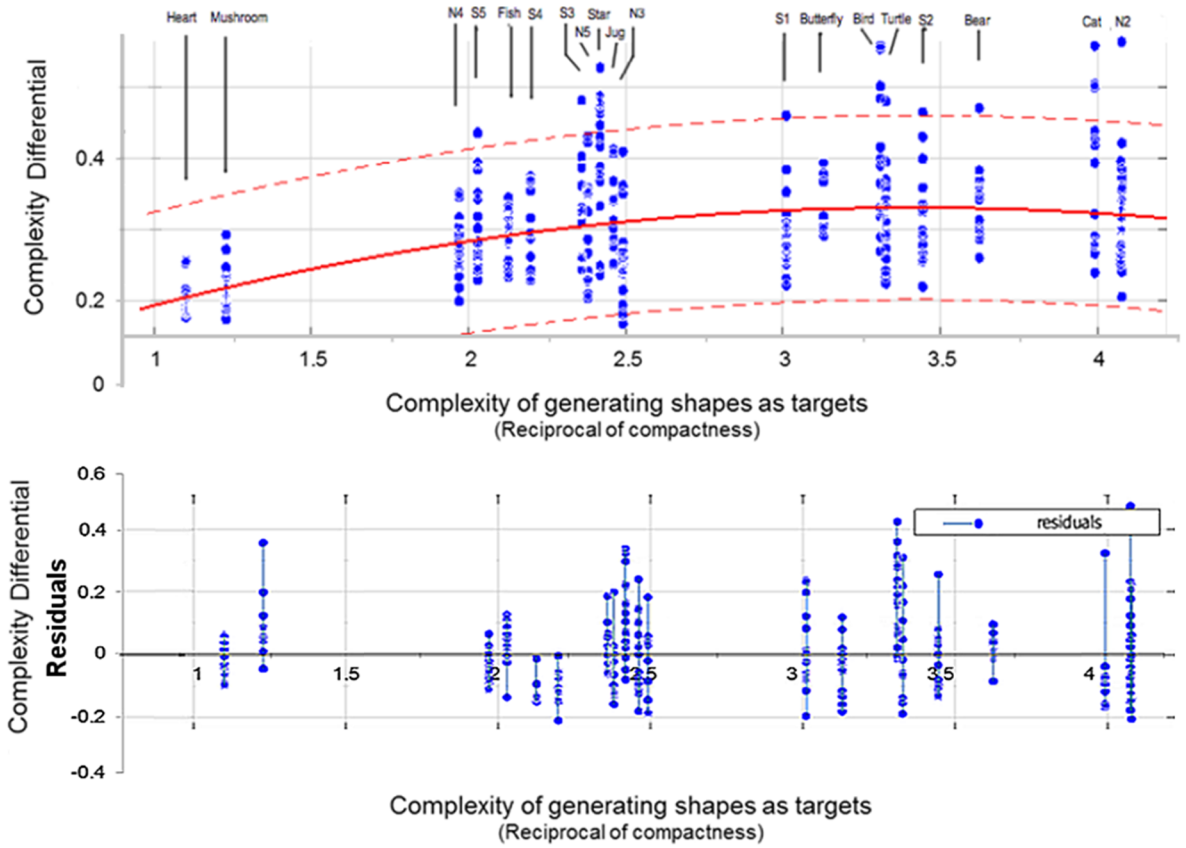

Fig. 17. The Complexity differential for individual contours as a function of the complexity of the initial contour shape in the control condition. The complexity differentials (y-axis) are presented against the initial complexity of the contour shape being detected (x-axis). The red line represents the method of least squares fit, while the broken red line represents the 95 percent prediction intervals. The lower graph presents the residual Complexity differentials compared with the estimated fit. (For interpretation of the references to colour in this figure legend, the reader is referred to the web version of this article.)

Alternatively, we can view the process of adding orientation noise as not simply disrupting the visibility of the implied contour, but rather that addition of noise implies a different, more (or less) complex shape. The facilitation effect under this scenario could be seen a one where the integrated contour is seen as being more or less likely representing a shape depending on its relationship with the flanker. The implication of such behaviour is that the visual system is performing contour integration first, and then, on the basis of additional evidence, accepting that this integrated contour is likely to indicate a 'real signal'.

4.1. Is the facilitation pre- or post-contour integration?

To determine whether the additional information afforded to the visual system is involved with either the actual contour integration (e.g., signal plays a role in local integration) or affects the visibility of a detectable contour (e.g., signal is used post-integration) it is worth remembering that, post-integration, additional cues are present from having a 'whole' contour such as shape complexity, aspect-ratio, symmetry, amongst others. These arise by virtue of combinations of factors such as interior area and boundary, and therefore are indicative of the contour integration processes having been achieved (post-contour integration). Hence, the addition of orientation noise jitter trial-by-trial has two effects – it increases the difficulty of integrating local links across the contour during the integration process, and it also has a global impact, post-integration – and makes the resulting 'whole' contour more complex after the local processing has resolved itself.

To investigate the role of change in complexity (compactness) a measure was developed that could distinguish between the initial complexity of the shape in the absence of orientation noise, and hence the intrinsic difficulty of detecting the shape contour even in the absence of noise, and the increase in complexity for that given shape due to the addition of noise jitter as observers reached their threshold detectability. We called this the Complexity Differential. This measure was based on two assumptions: (1) the gaborized contour target could still be treated as representing smooth shape even after the addition of orientation noise (2) the area within the contour remains constant with added noise (i.e., orientation noise would, on average, add and subtract the same area from within and without the initial contour shape leaving the average area the same regardless of orientation noise; see Fig. 5).

To relate orientation noise (the original dependent variable) to a measure of contour complexity change, the complexity differential was calculated by: (1) estimating the change in the complexity of a smooth contour caused per degree of orientation noise (2) using this value to calculate the complexity of the target contour at the detection threshold and (3) subtracting the complexity at threshold from the initial complexity of the generating contour. The resultant value corresponds to the putative change in complexity that occurs from initial suprathreshold contour to the smooth contour implied by fitting the jittered orientations of gabors at detection threshold (see Appendix B).

4.2. Recasting detection threshold in terms of contour complexity

The complexity differential was computed for each target shape and plotted as a function of the underlying complexity of the generating contour separately for the control (no Flanker) and matching flanker conditions in Figs. 17 and 18 respectively. Data points are for all observers tested. A least-squares quadratic polynomial fit was performed on the complexity differential as a function of the complexity of the shape used as the target contour (Using the Curve Fitting Toolbox in Matlab). A bi-square weight (Heiberger & Becker, 1992) was used to

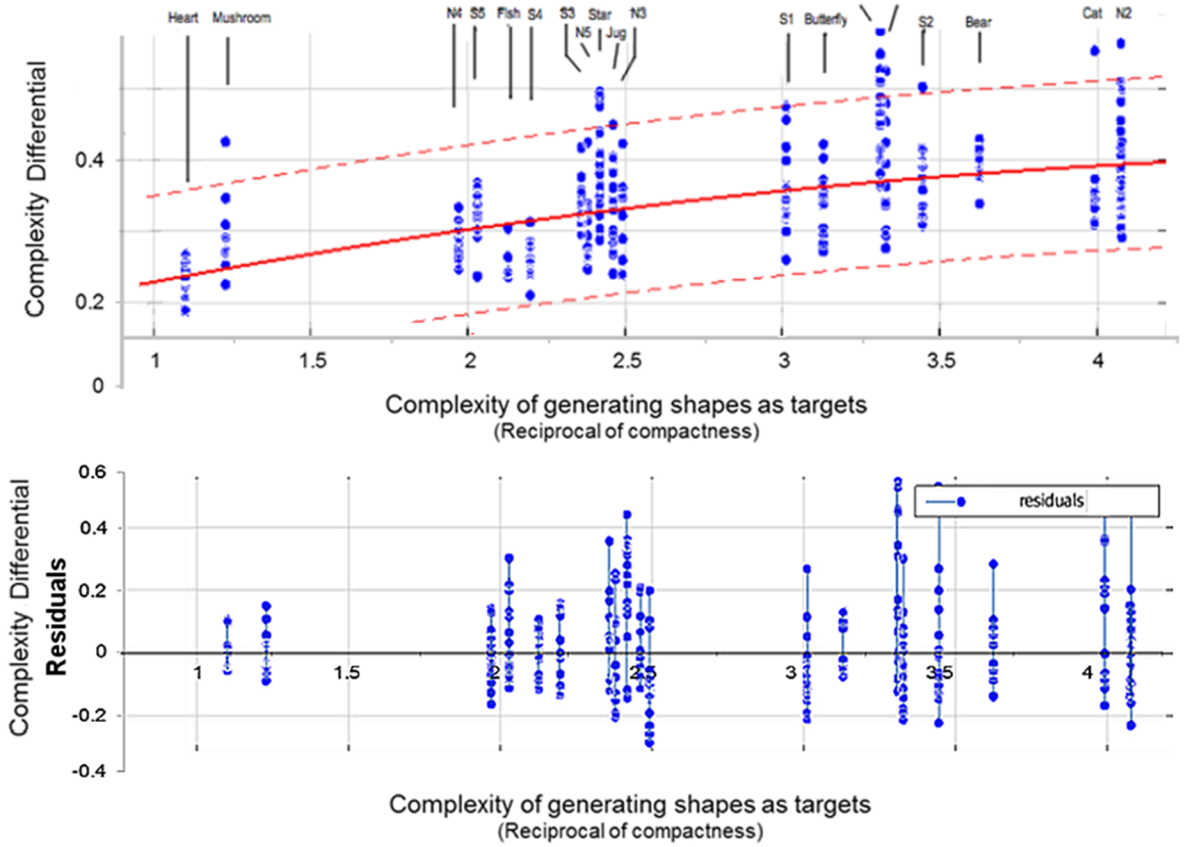

Fig. 18. The Complexity differential for individual contours as a function of the complexity of the initial contour shape in the Matching condition. The Complexity differential results (y-axis) are presented against the initial complexity of the contour shape being detected (x-axis). The red line represents the least squares fit, while the broken red line represents the 95 percent prediction intervals. The lower graph presents the residual Complexity differentials compared with the estimated fit. (For interpretation of the references to colour in this figure legend, the reader is referred to the web version of this article.)

minimise the effects of outliers. This method minimizes the effects of outliers by giving higher weighting to points near the centre line fit to the majority of the dataset and reducing the weight for each data point the further the data point is from the line.

In comparison with the plots where threshold were plotted in terms of orientation jitter (Figs. 15 and 16), there is a more systematic trend across the dataset when recast in terms complexity differentials (Figs. 17 and 18). This is true for both the control (No Flanker) and Matched Flanker conditions. In both conditions there is a general monotonic increase in the complexity differentials as a function of the initial complexity of the target shape. For the control condition, the method of least-squares fit was a quadratic (Degree 2) polynomial fit which had an R-squared value that accounted for 37.34 percent of the variation observed across the dataset. The root-mean-squared error for the fit was 0.1312.

The thresholds plotted as complexity differentials generally increased with increasing complexity of the base contour (in the range of C = 1–3). However, beyond this range the thresholds (complexity differentials for shapes with C > 3) decreased in magnitude. For the Matched Flanker condition, the fit was also a quadratic (degree 2) polynomial, and this fit had an R-squared value which accounted for 41.01 percent of the variation observed across the dataset. The root-

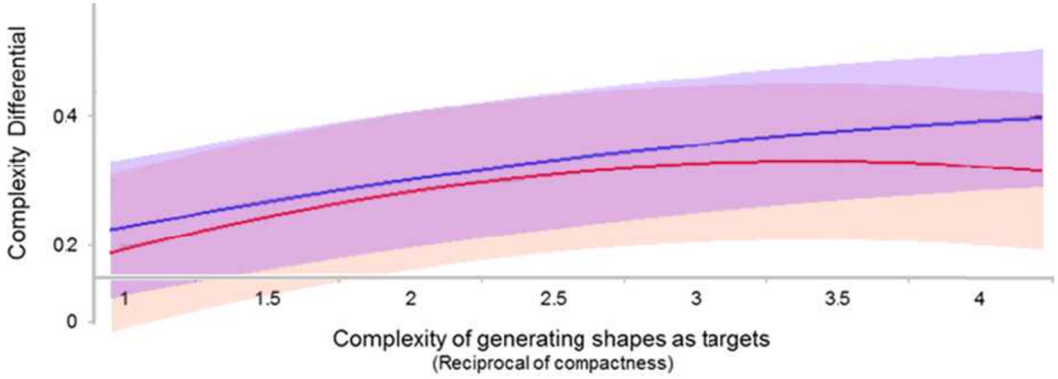

Fig. 19. Comparison of the quadratic fits of the complexity differential as a function of the complexity of the target contour in the control and Matching conditions. The Complexity differentials (y-axis) is plotted against the complexity of the target contour (x-axis) for the control (red) and Matching (blue) condition. The shaded regions are the 95% confidence intervals. The difference shows a trend in the data and was not statistically tested. (For interpretation of the references to colour in this figure legend, the reader is referred to the web version of this article.)

mean-squared error was 0.12. Unlike the control condition, in this case, the Complexity differentials showed a consistent monotonic increase even at the higher levels of shape complexity (C > 3).

4.3. Comparison of fits of the control and matching conditions

Fig. 19 plots both the regression curves obtained for the control (No-flanker) condition (Fig. 17) and the Matched Flanker condition (Fig. 18). When the curves are compared we can see that for both conditions the complexity differential increases more or less monotonically between complexity of 1 and 3 for both conditions. In addition, we see that detection performance in the matched flanker condition as captured by the complexity differential (blue line) is generally higher by a similar amount for most values of underlying contour complexity. While this difference between the two curves falls well within the 95% confidence intervals, the consistent shift between the two suggests that the effect of flankers is in some way systematically tied to the complexity of the target (flanker) shapes.

4.4. Interpretation

Our results are suggestive of the fact that the facilitation is consistent with the independent impact of the orientation noise on the complexity of the whole shape. Hence it would be consistent with a model that first spontaneously integrates contours with the subsequent integration of flanker information used to compute the likelihood of the contour signal indicating a real object; in turn the contour becomes more likely and, hence, more visible. This is consistent with previous research which has indicated that complexity related cues – interior area and boundary length (Machilsen & Wagemans, 2011) – are relevant to the detection of contours.

In summary, the shape level flanker facilitation observed suggests that the information from the flankers is a feedback process into perceptual mechanisms responsible for contour integration rather than simply acting as a top-down search template.

One final aspect of the data is that the presence of symmetry amplified the magnitude of the facilitation observed within the conditions. This may indicate that the shape-level flanker facilitation effect is exactly this – a shape-level effect in which all relevant features within the flankers are useful to the more local integration of the contour. However, there are reasons to be cautious with this interpretation. Firstly, studies have demonstrated that bilateral symmetry does not aid in the detection of peripheral Gaborized contours (Machilsen et al., 2009; Sassi et al., 2014). Secondly, the presence of bilateral symmetry may be introducing a methodological confound in the form of contextual inter-contour symmetries (i.e., symmetries between adjacent contour sections between objects). These inter-object symmetries have already been linked to the detection of multiple objects (Baylis & Driver, 1995, 2001; Bertamini, 2010; Koning & Wagemans, 2009; van der Helm & Treder, 2009). Hence, rather than an additional shape-level process it may also indicate a secondary more local lateral interaction between adjacent lengths of contours.

Acknowledgement

This work by funded by an EPSRC doctoral training grant at the University of St Andrews, Scotland.

Commercial interests: None.

Appendix A. Complexity values of contour shapes

The shapes used to generate each contour were grouped together by the absence or presence of specific features (bilateral symmetry, familiarity). However, owing to the range of possible differences between each shape it was necessary to control for the overall complexity of shapes within each group. The absolute length of the boundary of each shape was recorded, as was the interior area within this boundary. These values were then used to calculate the complexity of each shape with respect to a circle. These values are shown in the table below. The magnitude of the complexity value of a shape was calculated using the reciprocal of the equation typically used to define shape compactness. Compactness is inversely proportional to the length of perimeter given the area, while complexity is directly proportional to the perimeter given the area. The index value of both measures is the circle as this shape has the property of having the maximum amount of area for the least amount of perimeter (thus the lowest complexity and the highest compactness).

The equation for complexity used for this experiment is C = (P^2)/(4 * PI^2 * A), where C is complexity, P is the absolute perimeter length, and A is the enclosed area

A.1. Table of complexity values

The table below contains the values for each shape used. Note that the perimeter and area were formulated from the initial .svg file in Inkscape and neither the area nor perimeter correspond to the scaled versions presented within the experiment. Complexity is independent of scale and therefore remains unchanged after rescaling. As both perimeter and area vary in the sample shapes, complexity is not necessarily monotonically related to the perimeter length.

Shape name	Perimeter length, mm	Area, mm^2	Complexity, C (Dimensionless)
Mushroom	264.16	4519.09	1.229
Heart	287	5954	1.101
Fish	324.12	3931.78	2.127
S5	326.55	4183.49	2.029
Star	332	3628	2.419
Bird	339.58	2773.19	3.311
N4	360.84	5262.46	1.970
N5	369	4554.75	2.380
N3	393.78	4954.42	2.492
Turtle	396.17	3754.99	3.328
S4	402.5	5868.16	2.198
S3	405.44	5544.98	2.360
Jug	412.2	5495.71	2.462
S1	418.39	4628.7	3.011
Bear	424.22	3589.03	3.992
N2	428.62	3586.45	4.078

N1	438.17	4437.37	3.445
Cat	464.37	4213.12	4.075
S2	465.11	4751.1	3.625
Butterfly	494.48	6219.9	3.130

Appendix B. Is the facilitation effect global or local?

B.1. Aim

The independent variable, orientation noise jitter, is a measure of the local change to the orientation of individual Gabor patches. It does not capture the effect of such local changes on the apparent shape of the integrated contour. Using the measurement of shape complexity, the orientation noise jitter is recast as a measurement of the change in the complexity from base shape to shape defined by orientation jitter at threshold (the complexity differential). This was done to determine whether any changes to the contour during the experiment occurs at a local or global level.

B.2. Description

The introduction of flanking contours was found to be facilitative to the integration of a closed contour. The facilitation of a contour may provide either local (pre-integration, Gabor orientation/position/alignment) or global (post-integration, likely distribution/aspect ratio) information to the target region.

In addition to the target and flanker shapes, noise threshold, and the presence of features we also have a pre-experiment measurement of the complexity of the underlying shape used to generate the Gaborized contour (see Appendix C). This additional information concerns the relative disruption of absolute perimeter length and area.

In the context of our experiment we are interested in establishing whether the performance of the participants per individual contour can be accounted for by the properties of the entire contour (hence, a global detection process). And, if so, does the increase in the facilitation arise because of global processes, or simply because the visual system is more robust to noise?

B.3. Is complexity an appropriate measurement to distinguish between the two cases?

The equation that represents complexity has a number of properties and assumptions that are useful for the purposes of determining whether facilitation is global or local.

(1) The measurement pre-supposes a continuous perimeter which can be quantified as an absolute value.

In the context of the experiment, the detection of a continuous, closed perimeter is post-integration (as by definition, there is no closed contour until contour integration has occurred). Hence, the value is useful to determine whether the participant is detecting a whole, closed contour up to the noise threshold, or a statistical arrangement of disconnected features that eventually is indistinguishable from the statistical features of the noise background.

(2) The measurement is dimensionless and is insensitive to differences in size and specific or anomalous features within a shape.

Variation can occur in the stimuli set due to having contours that must have certain features preserved to be identifiable or symmetric. This introduces additional noise into the dataset as the area and perimeter, and specific features of the shapes may vary even after being scaled. In addition, as the index ($C = 1$) is a circle the measurement can be interpreted relative to a known feature (circularity), thus the entire dataset can be compared and any non-linearity more readily identified.

Hence, as a ratio of area/perimeter length, the complexity of the target shape requires that the detection of an entire closed contour is taking place as well as allowing comparisons between shapes.

B.4. What experimental factors are resolved if we use complexity?

The experimental task involves the addition of some range of randomised noise to the local orientation of the Gabor patches aligned to the contours shape. The participant is asked to distinguish between one of two panels, one of which is wholly randomised.

There exists a confound in the methodology in which a person could perceive a statistical property of one panel rather than a closed contour. In other words, the person may be sensitive to differences in absolute area/perimeter or slight statistical differences between one panel and the next. Hence, the orientation noise could be considered as introducing a statistically disruptive effect on the whole panel, rather than breaking contour integration.

This implies that:

(1) If orientation jitter is a good measurement of the detection of a closed contour (not effected by non-linear behaviours) the noise threshold will be monotonically related to its underlying complexity of the target.
(2) If orientation jitter captures additional factors that lead to the breaking of closure (sensitivities to specific local features, variation in sizes of target, or statistical features) then the resulting noise threshold will vary more greatly and will vary non-monotonic with the underlying complexity of the target.

One way of getting around this issue is to recast the orientation noise as the absolute change in complexity (Complexity differential). Hence the values will be a function of changes to the closed contour, rather than a simple ranged value that increases linearly.

The complexity differential therefore constitutes a way of determining whether the complexity of the initial shape of the target is monotonically

related to the results. The value is also a measurement of a global change with each degree of noise added, and hence, will provide evidence about whether the degree of facilitation is linked to the visual system using global or local information.

B.5. General description of methodology to calculate the complexity differential

Consequently, the change in complexity can be found by:

(A) Determining the change in the absolute perimeter length for each degree of orientation jitter added to the contour.
(B) Calculating the compactness value of the target at the noise threshold.
(C) Subtracting the initial complexity value from the complexity value at the threshold.

This will then result in a value corresponding to the magnitude of the change of the complexity when the contour is no longer visible. This can then be compared against the initial complexity value of each target to determine whether, overall, the degree of change is directly related to the initial complexity of the target. And furthermore, whether the flanking contours contribute to this process. Hence, the detection performance will be directly linked to the shape level properties of the contour, rather than the discrimination of differences between two panels of varying randomisation.

Appendix C. The complexity differential

C.1. Methodology

The initial contours used a vector representation which traced out the initial shape. To determine the compactness, a native application in Inkscape was used to make measurements of the length of the shapes contour and the area that it enclosed.

Two reference Gaborized shapes were chosen – a Circle and a Butterfly. Splines for a vector shape were manually matching to the reference shapes. Correspondingly, a set of 3 Gaborized versions of these shapes (That is, the version that were be shown during each trial) at 5 different levels of orientation jitter (50, 70, 90, 110 deg of orientation jitter) were placed under the vector shapes.

The individual splines of the vector shape were aligned to the Gabor patches under increasing degrees of noise. This produced a vector shape that corresponded with a smooth shape given the local values of the orientated Gabor patches. This new contour length and area was measured for the shapes with larger amounts of orientation noise. The average change to the contour length for 1 degree of noise was calculated. This number was used to convert the detection thresholds into absolute values concerning the overall change to the compactness for the increase in orientation noise jitter.

Each degree of noise can produce indents and extrusions along the contour. It was assumed that these would be roughly equal, and thus the initial area would be preserved for a single contour. In addition, that experimentally, deviations from a constant area would be evident in the data.

(A) This resulted in the relationship:

$$\Delta P = 0.4 * n \tag{1.2}$$

where ΔP is the change of complexity, and n is the noise threshold.

An important factor to note here is that the maximum range of noise (180) results would result in additional of 72 mm of perimeter. Whereas the range of perimeters is 264–494. Hence even at maximum the contribution to the perimeter will be between +27% and +14% respectively. Hence, in terms of complexity the initial perimeter contributes more than the additional perimeter due to the addition of orientation noise. This reflects the fact that before orientation noise is added to the contour each shape has varying complexity but equal visibility.

(B) The compactness value was calculated by:

$$C = \frac{(P + \Delta P)^2}{4 * \pi * A} \tag{1.3}$$

where C is the Compactness at the noise threshold, P is the Absolute perimeter of the initial contour, ΔP is the additional perimeter at the noise threshold, and A is the Area within the boundary contour.

Below is a comparison between changes to the perimeter of two shapes of varying complexity with respect to the numerator of the equation (Perimeter squared).

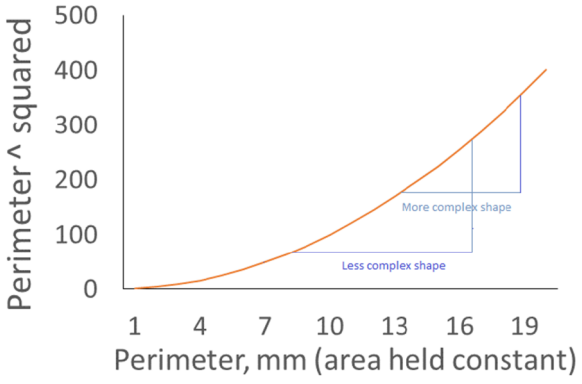

An important note is that this relationship can preserve the initial order of complexity. That is, because the initial perimeter determines the

relationship more than the additional perimeter even if a simpler shape has more noise threshold, it may still result in a simpler shape ending up with a final complexity value that is less than that of a non-complex shape.

To account for this counter-intuitive result note that the orientation noise confounds contour detection with interactions within the noise field. Hence, if this factor is significant in the results it represents a limiting factor on the degree complexity a contour can have before closure is broken.

(C) Finally, the complexity differential was calculated as:

$$C_d = C_2 - C_1 \tag{1.3}$$

This value captures the difference between the initial and final complexity at the point at the contour is no longer visible.

References

Alvarez, G. A. (2011). Representing multiple objects as an ensemble enhances visual cognition. *Trends in Cognitive Sciences, 15*(3), 122–131. https://doi.org/10.1016/j.tics.2011.01.003.

Alvarez, G. A., & Oliva, A. (2008). The representation of simple ensemble visual features outside the focus of attention. *Psychological Science, 19*(4), 392–398. https://doi.org/10.1111/j.1467-9280.2008.02098.x.

Ariely, D. (2001). Seeing sets: Representation by statistical properties. *Psychological Science, 12*(2), 157–162. https://doi.org/10.1111/1467-9280.00327.

Attneave, F. (1954). Some informational aspects of visual perception. *Psychological Review, 61*(3), 183–193. https://doi.org/10.1037/h0054663.

Barlow, H. B., & Reeves, B. C. (1979). Versatility and absolute efficiency of detecting mirror symmetry in random dot displays. *Vision Research, 19*(7), 783–793. https://doi.org/10.1016/0042-6989(79)90154-8.

Baylis, G. C., & Driver, J. (1989). Movement and visual-attention – The spotlight metaphor breaks down. *Journal of Experimental Psychology-Human Perception and Performance, 15*(3), 448–456.

Baylis, G. C., & Driver, J. (1992). Visual parsing and response competition – The effect of grouping factors. *Perception & Psychophysics, 51*(2), 145–162. https://doi.org/10.3758/bf03212239.

Baylis, G. C., & Driver, J. (1995). Obligatory edge assignment in vision: The role of figure and part segmentation in symmetry detection. *Journal of Experimental Psychology: Human Perception and Performance, 21*, 1323–1342.

Baylis, G. C., & Driver, J. (2001). Perception of symmetry and repetition within and across visual shapes: Part-based descriptions and object-based attention. *Visual Cognition, 8*, 163–196.

Beck, J., Rosenfield, A., & Avry, R. (1989). Line segregation. *Spatial Vision, 4*, 75–101.

Ben-David, B. M., & Algom, D. (2009). Species of redundancy in visual target detection. *Journal of Experimental Psychology-Human Perception and Performance, 35*(4), 958–976. https://doi.org/10.1037/a0014511.

Bertamini, M. (2010). Sensitivity to reflection and translation is modulated by objectness. *Perception, 39*(1), 27–40. https://doi.org/10.1068/p6393.

Bertamini, M., & Farrant, T. (2005). Detection of change in shape and its relation to part structure. *Acta Psychologica, 120*(1), 35–54. https://doi.org/10.1016/j.actpsy.2005.03.002.

Bertamini, M., & Wagemans, J. (2013). Processing convexity and concavity along a 2-d contour: Figure-ground, structural shape, and attention 213. *Psychonomic Bulletin & Review, 20*(2), 191–207. https://doi.org/10.3758/s13423-012-0347-2.

Born, R. (2000). Center-surround interactions in the middle temporal visual area of the owl monkey. *Journal of Neurophysiology, 84*(5), 2658–2669.

Bouma, H. (1970). Interaction effects in parafoveal letter recognition. *Nature, 226*(5241), 177. https://doi.org/10.1038/226177a0.

Brainard, D. (1997). The psychophysics toolbox. *Spatial Vision, 10*(4), 433–436. https://doi.org/10.1163/156856897x00357.

Bundesen, C., Habekost, T., & Kyllingsbaek, S. (2005). A neural theory of visual attention: Bridging cognition and neurophysiology. *Psychological Review, 112*(2), 291–328. https://doi.org/10.1037/0033-295x.112.2.291.

Carrasco, M., Ling, S., & Read, S. (2004). Attention alters appearance. *Nature Neuroscience, 7*(3), 308–313. https://doi.org/10.1038/nn1194.

Cass, J., & Spehar, B. (2005). Dynamics of collinear contrast facilitation are consistent with long range horizontal striate transmission. *Vision Research, 45*(21), 2728–2739. https://doi.org/10.1016/j.visres.2005.03.010.

Chen, C., & Tyler, C. (2001). Lateral sensitivity modulation explains the flanker effect in contrast discrimination. *Proceedings of the Royal Society B: Biological Sciences, 268*(1466), 509–516.

Chong, S., & Treisman, A. (2003). Representation of statistical properties. *Vision Research, 43*(4), 393–404. https://doi.org/10.1016/s0042-6989(02)00596-5.

Dakin, S., & Watt, R. (1997). The computation of orientation statistics from visual texture. *Vision Research, 37*(22), 3181–3192. https://doi.org/10.1016/s0042-6989(97)00133-8.

Demeyer, M., & Machilsen, B. (2012). The construction of perceptual grouping displays using GERT. *Behavior Research Methods, 44*(2), 439–446. https://doi.org/10.3758/s13428-011-0167-8.

Desimone, R., & Duncan, J. (1995). Neural mechanisms of selective visual-attention. *Annual Review of Neuroscience, 18*, 193–222. https://doi.org/10.1146/annurev.neuro.18.1.193.

Duncan, J. (1984). Selective attention and the organization of visual information. *Journal of Experimental Psychology-General, 113*(4), 501–517. https://doi.org/10.1037/0096-3445.113.4.501.

Elder, J., & Zucker, S. (1993). The effect of contour closure on the rapid discrimination of 2 dimensional shapes. *Vision Research, 33*(7), 981–991. https://doi.org/10.1016/0042 6989(93)90080-g.

Evans, K. K., Horowitz, T. S., Howe, P., Pedersini, R., Reijnen, E., Pinto, Y., & Wolfe, J. M. (2011). Visual attention. *Wiley Interdisciplinary Reviews-Cognitive Science, 2*(5), 503–514. https://doi.org/10.1002/wcs.127.

Field, D., Hayes, A., & Hess, R. (1993). Contour integration by the human visual-system – Evidence for a local association field. *Vision Research, 33*(2), 173–193. https://doi.org/10.1016/0042 6989(93)90156-q.

Freeman, E., Sagi, D., & Driver, J. (2001). Lateral interactions between targets and flankers in low level vision depend on attention to the flankers. *Nature Neuroscience, 4*(10), 1032–1036. https://doi.org/10.1038/nn728.

Friedenberg, J., & Bertamini, M. (2000). Contour symmetry detection: The influence of axis orientation and number of objects. *Acta Psychologica, 105*, 107–118.

Gerhardstein, P., Tse, J., Dickerson, K., Hipp, D., & Moser, A. (2012). The human visual system uses a global closure mechanism. *Vision Research, 71*, 18–27. https://doi.org/10.1016/j.visres.2012.08.011.

Heiberger, R, & Becker, R. (1992). Design of an s-function for robust regression using iteratively reweighted least-squares. In H. J. Newton (Ed.), Computing Science and Statistics: Vol 24: Graphics and Visualization (p. 112–116). Fairfax: Interface Foundation North America. (24th Symposium on the interface of computing science and statistics: graphics and visualization, College Station, TX, Mar 18–21, 1992).

Hoffman, D., & Singh, M. (1997). Salience of visual parts. *Cognition, 63*(1), 29–78.

Huang, P. C., & Hess, R. F. (2007). Collinear facilitation: Effect of additive and multiplicative external noise. *Vision Research, 47*(24), 3108–3119. https://doi.org/10.1016/j.visres.2007.08.007.

Hubel, D., & Wiesel, T. (1959). Receptive fields of single neurones in the cats striate cortex. *Journal of Physiology, 148*(3), 574–591.

Hubel, D., & Wiesel, T. (1962). Receptive fields, binocular interaction and functional architecture in cats visual cortex. *Journal of Physiology, 160*(1), 106–1000.

Huttenlocher, D., & Wayner, P. (1992). Finding convex edge groupings in an image. *International Journal of Computer Vision, 8*(1), 7–27. https://doi.org/10.1007/bf00126398.

Jolicoeur, P., & Milliken, B. (1989). Identification of disoriented objects – Effects of context of prior presentation. *Journal of Experimental Psychology-Learning, Memory and Cognition, 15*(2), 200–210. https://doi.org/10.1037/0278-7393.15.2.200.

Kaernbach, C. (1991). Simple adaptive testing with the weighted up-down method. *Perception & Psychophysics, 49*(3), 227–229. https://doi.org/10.3758/bf03214307.

Kanizsa, G. (1976). Subjective contours. *Scientific American, 234*(4), 48–52.

Keane, S., Hayward, W., & Burke, D. (2003). Detection of three types of changes to novel objects. *Visual Cognition, 10*(1), 101–127. https://doi.org/10.1080/13506280143000014.

Koenderink, J., & Van Doorn, A. (1979). Internal representation of solid shape with respect to vision. *Biological Cybernetics, 32*(4), 211–216. https://doi.org/10.1007/bf00337644.

Koffka, K. (1935). *Principles of Gestalt psychology.* London: Lund Humphries.

Koning, A., & Wagemans, J. (2009). Detection of symmetry and repetition in one and two objects structures versus strategies. *Experimental Psychology, 56*(1), 5–17. https://doi.org/10.1027/1618-3169.56.1.5.

Kovacs, I., & Julesz, B. (1993). A closed curve is much more than an incomplete one – Effect of closure in figure ground segmentation. *Proceedings of the National Academy of Sciences of the United States of America, 90*(16), 7495–7497. https://doi.org/10.1073/pnas.90.16.7495.

Kravitz, D. J., & Behrmann, M. (2011). Space-, object-, and feature-based attention interact to organize visual scenes. *Attention Perception & Psychophysics, 73*(8), 2434–2447. https://doi.org/10.3758/s13414-011-0201-z.

Krummenacher, J., Muller, H., & Heller, D. (2001). Visual search for dimensionally redundant pop out targets: Evidence for parallel-coactive processing of dimensions. *Perception & Psychophysics, 63*(5), 901–917. https://doi.org/10.3758/bf03194446.

Krummenacher, J., Muller, H., & Heller, D. (2002a). Visual search for dimensionally redundant pop out targets: Parallel-coactive processing of dimensions is location specific. *Journal of Experimental Psychology-Human Perception and Performance, 28*(6), 1303–1322. https://doi.org/10.1037//0096-1523.28.6.1303.

Krummenacher, J., Muller, H., & Heller, D. (2002b). Visual search for dimensionally redundant pop out targets: Redundancy gains in compound tasks. *Visual Cognition, 9*(7), 801–837. https://doi.org/10.1080/13506280143000269.

Levin, D., & Simons, D. (1997). Failure to detect changes to attended objects in motion pictures. *Psychonomic Bulletin & Review, 4*(4), 501–506. https://doi.org/10.3758/bf03214339.

Loffler, G. (2008). Perception of contours and shapes: Low and intermediate stage mechanisms. *Vision Research, 48*(20), 2106–2127. https://doi.org/10.1016/j.visres.2008.03.006.

Mach, E. (1885/1959). *The analysis of sensations.* New York: Dover.

Machilsen, B., Pauwels, M., & Wagemans, J. (2009). The role of vertical mirror symmetry in visual shape detection. *Journal of Vision, 9*(12), https://doi.org/10.1167/9.12.11.

Machilsen, B., & Wagemans, J. (2011). Integration of contour and surface information in shape detection. *Vision Research, 51*(1), 179–186. https://doi.org/10.1016/j.visres.2010.11.005.

Machilsen, B., Wagemans, J., & Demeyer, M. (2016). Quantifying density cues in

grouping displays. *Vision Research, 126*, 207–219. https://doi.org/10.1016/j.visres.2015.06.004.
Marcelja, S. (1980). Mathematical-description of the responses of simple cortical-cells. *Journal of the Optical Society of America, 70*(11), 1297–1300. https://doi.org/10.1364/josa.70.001297.
Martinez, A., Ramanathan, D. S., Foxe, J. J., Javitt, D. C., & Hillyard, S. A. (2007). The role of spatial attention in the selection of real and illusory objects. *Journal of Neuroscience, 27*(30), 7963–7973. https://doi.org/10.1523/jneurosci.0031-07.2007.
Maxfield, I. (1997). Attention and semantic priming: A review of prime task effects. *Consciousness and Cognition, 6*(2–3), 204–218. https://doi.org/10.1006/ccog.1997.0311.
Mcmains, S., & Somers, D. (2004). Multiple spotlights of attentional selection in human visual cortex. *Neuron, 42*(4), 677–686. https://doi.org/10.1016/s0896-6273(04)00263-6.
Miller, J. (1982). Divided attention – Evidence for co-activation with redundant signals. *Cognitive Psychology, 14*(2), 247–279. https://doi.org/10.1016/0010-0285(82)90010-x.
Montero, R., & Bribiesca, E. (2009). State of the art of compactness and circularity measures. *International Mathematical Forum, 4*(27), 1305–1335.
Moses, Y., Ullman, S., & Edelman, S. (1996). Generalization to novel images in upright and inverted faces. *Perception, 25*(4), 443–461. https://doi.org/10.1068/p250443.
Mundy, M. E., Honey, R. C., & Dwyer, D. M. (2007). Simultaneous presentation of similar stimuli produces perceptual learning in human picture processing. *Journal of Experimental Psychology-Animal Behavior Processes, 33*(2), 124–138. https://doi.org/10.1037/0097-7403.33.2.124.
Mundy, M. E., Honey, R. C., & Dwyer, D. M. (2009). Superior discrimination between similar stimuli after simultaneous exposure. *Quarterly Journal of Experimental Psychology, 62*(1), 18–25. https://doi.org/10.1080/17470210802240614.
Nygard, G. E., Sassi, M., & Wagemans, J. (2011). The influence of orientation and contrast flicker on contour saliency of outlines of everyday objects. *Vision Research, 51*(1), 65–73. https://doi.org/10.1016/j.visres.2010.09.032.
Olivers, C. N. L., Peters, J., Houtkamp, R., & Roelfsema, P. R. (2011). Different states in visual working memory: When it guides attention and when it does not. *Trends in Cognitive Sciences, 15*(7), 327–334. https://doi.org/10.1016/j.tics.2011.05.004.
Palmer, S., Rosch, E. & Chase, P. (1981). Canonical perspective and the perception of objects. (vol. ix; J. Long & A. Baddeley, Eds.). Hillsdale, NJ: Lawrence Erlbaum.
Pashler, H. (1994). Dual-task interference in simple tasks – Data and theory. *Psychological Bulletin, 116*(2), 220–244. https://doi.org/10.1037/0033-2909.116.2.220 223.
Pelli, D. G., & Tillman, K. (2008). The uncrowded window of object recognition. *Nature Neuroscience, 11*(10), 1129–1135. https://doi.org/10.1038/nn.2187.
Petrov, Y., Popple, A. V., & Mckee, S. P. (2007). Crowding and surround suppression: Not to be confused. *Journal of Vision, 7*(2), https://doi.org/10.1167/7.2.12.
Polat, U., & Sagi, D. (1993). Lateral interactions between spatial channels – Suppression and facilitation revealed by lateral masking experiments. *Vision Research, 33*(7), 993–999. https://doi.org/10.1016/0042-6989(93)90081-7.
Posner, M., Snyder, C., & Davidson, B. (1980). Attention and the detection of signals. *Journal of Experimental Psychology-General, 109*(2), 160–174. https://doi.org/10.1037//0096-3445.109.2.160.
Prins, N. & Kingdom, F. (2001). Palamedes: Matlab routines for analyzing psychophysical data. Retrieved from www.palamedestoolbox.org.
Pylyshyn, Z. W., & Storm, R. W. (1988). Tracking multiple independent targets evidence for a parallel tracking mechanism. *Spatial Vision, 3*(3), 179–198.
R Development Core Team (2008). R: A language and environment for statistical computing [computer software manual]. Vienna, Austria.
Regan, D., & Hamstra, S. (1992). Shape-discrimination and the judgment of perfect symmetry dissociation of shape from size. *Vision Research, 32*(10), 1845–1864. https://doi.org/10.1016/0042-6989(92)90046-l.
Rensink, R., O'Regan, J., & Clark, J. (1997). To see or not to see: The need for attention to perceive changes in scenes. *Psychological Science, 8*(5), 368–373. https://doi.org/10.1111/j.1467 9280.1997.tb00427.x.
Sassi, M., Demeyer, M., & Wagemans, J. (2014). Peripheral contour grouping and saccade targeting: The role of mirror symmetry. *Symmetry-Basel, 6*(1), 1–22. https://doi.org/10.3390/sym6010001.
Sassi, M., Machilsen, B., & Wagemans, J. (2012). Shape detection of gaborized outline versions of everyday objects. *i-perception, 3*(10), 745–764. https://doi.org/10.1068/i0499.
Sassi, M., Vancleef, K., Machilsen, B., Panis, S., & Wagemans, J. (2010). Identification of everyday objects on the basis of gaborized outline versions. *i-perception, 1*(3), 121–142. https://doi.org/10.1068/i0384.
Smits, J. T., Vos, P. G., & van Oeffelen, M. P. (1985). The perception of a dotted line in noise: a model of good continuation and some experimental results. Retrieved from *Spatial Vision, 1*(2), 163–177. http://booksandjournals.brillonline.com/content/journals/10.1163/156856885x00170.
Stojanoski, B., & Niemeier, M. (2007). Feature-based attention modulates the perception of object contours. *Journal of Vision, 7*(14), https://doi.org/10.1167/7.14.18.
Stuart, J., & Burian, H. M. (1962). Study of separation difficulty – Its relationship to visual acuity in normal and amblyopic eyes. *American Journal of Ophthalmology, 53*(3), 471–1000.
Tarr, M., & Pinker, S. (1989). Mental rotation and orientation dependence in shape-recognition. *Cognitive Psychology, 21*(2), 233–282. https://doi.org/10.1016/0010-0285(89)90009-1.
Todd, J. (1912). Reaction to multiple stimuli. *Archives of Psychology, 2*, 1–65.
Toet, A., & Levi, D. (1992). The 2-dimensional shape of spatial interaction zones in the parafovea. *Vision Research, 32*(7), 1349–1357. https://doi.org/10.1016/0042-6989(92)90227-a.
Treder, M. S. (2010). Behind the looking-glass: A review on human symmetry perception. *Symmetry-Basel, 2*(3), 1510–1543. https://doi.org/10.3390/sym2031510.
Tünnermann, J., Born, C. & Mertsching, B. (2013). Top-down visual attention with complex templates. In VISAPP 2013 - Proceedings of the international conference on computer vision theory and applications (p. 1).
van der Helm, P. A., & Leeuwenberg, E. (2004). Holographic goodness is not that bad: Reply to Olivers, Chater and Watson (2004). *Psychological Review, 111*(1), 261–273. https://doi.org/10.1037/0033-295x.111.1.261.
van der Helm, P. A., & Leeuwenberg, E. (1996). Goodness of visual regularities: A non-transformational approach. *Psychological Review, 103*(3), 429–456. https://doi.org/10.1037/0033-295x.103.3.429.
van der Helm, P. A., & Treder, M. S. (2009). Detection of (anti)symmetry and (anti) repetition: Perceptual mechanisms versus cognitive strategies. *Vision Research, 49*(23), 2754–2763. https://doi.org/10.1016/j.visres.2009.08.015.
Vetter, T., & Poggio, T. (1994). Symmetrical 3d objects are an easy case for 2d object recognition. *Spatial Vision, 8*(4), 443–453. https://doi.org/10.1163/156856894x00107.
Wagemans, J. (1995). Detection of visual symmetries. *Spatial Vision, 9*(1), 9–32. https://doi.org/10.1163/156856895x00098.
Wagemans, J., Elder, J. H., Kubovy, M., Palmer, S. E., Peterson, M. A., Singh, M., & Von Der Heydt, R. (2012). *Psychological Bulletin, 138*(6), 1172–1217. https://doi.org/10.1037/a0029333.
Wallach, H. (1935). Uber visuell wahrgenommene bewegungsrichtung. *Psychologische Forschung, 20*, 325–380.
Wertheimer, M. (1923). Studies concerning the theory of shape. *Psychologische Forschung, 4*, 301–350. https://doi.org/10.1007/bf00410640.
Williams, T. & Kelley, C. (2011). Gnuplot 4.5: An interactive plotting program.
Woods, R., Nugent, A., & Peli, E. (2002). Lateral interactions: Size does matter. *Vision Research, 42*(6), 733–745. https://doi.org/10.1016/s0042-6989(01)00313-3.
Wright, D., Makin, A., & Bertamini, M. (2017). Electrophysiological responses to symmetry presented in the left or in the right visual hemifield. *Cortex, 86*(2017), 93–108.
Yantis, S. (1992). Multielement visual tracking – Attention and perceptual organization. *Cognitive Psychology, 24*(3), 295–340. https://doi.org/10.1016/0010-0285(92)90010-y.
Yarbus, A. (1961). Eye movements during examination of complicated objects. *Biophysic-ussr, 6*(2), 52.
Zusne, l., & Michels, K. (1962a). Geometricity of visual form. *Perceptual and Motor Skills, 14*(1), 147–154.
Zusne, l., & Michels, K. (1962b). More on the geometricity of visual form. *Perceptual and Motor Skills, 15*(1), 55–58.